Software Defined Batteries

Anirudh Badam[1], Ranveer Chandra[1], Jon Dutra[1], Anthony Ferrese[2], Steve Hodges[1], Pan Hu[3], Julia Meinershagen[1], Thomas Moscibroda[1], Bodhi Priyantha[1], Evangelia Skiani[4]

[1]Microsoft Corporation, [2]Tesla Motors, [3]University of Massachusetts Amherst, [4]Columbia University

Abstract

Different battery chemistries perform better on different axes, such as energy density, cost, peak power, recharge time, longevity, and efficiency. Mobile system designers are constrained by existing technology, and are forced to select a single chemistry that best meets their diverse needs, thereby compromising other desirable features. In this paper, we present a new hardware-software system, called Software Defined Battery (SDB), which allows system designers to integrate batteries of different chemistries. SDB exposes APIs to the operating system which control the amount of charge flowing in and out of each battery, enabling it to dynamically trade one battery property for another depending on application and/or user needs. Using microbenchmarks from our prototype SDB implementation, and through detailed simulations, we demonstrate that it is possible to combine batteries which individually excel along different axes to deliver an enhanced collective performance when compared to traditional battery packs.

1. Introduction

The utility of a mobile device is often constrained by the capabilities of its battery. Whilst integrated circuit performance has doubled every eighteen months according to Moore's law, the same is far from true for battery technology. Battery performance can be evaluated in many different ways (see Table 1), but no matter which metric we look at, it has taken more than a decade to double performance.

Furthermore, the various properties of batteries are often at odds with each other. For example, batteries with higher power densities tend to have lower volumetric and gravimetric energy densities, and vice versa. Similarly, making a conformable battery that fits a particular industrial design compromises its performance characteristics.

SOSP'15, October 4–7, 2015, Monterey, CA.

http://dx.doi.org/10.1145/nnnnnnn.nnnnnnn

Battery Characteristic	**Units**
Energy capacity	Joule
Volume	mm^3
Mass	kilogram
Discharge rate	watt
Recharge rate	watt
Gravimetric energy density	joule / kilogram
Volumetric energy density	joule / liter
Cost	$ / joule
Discharge power density	watt / kilogram
Recharge power density	watt / kilogram
Cycle count	Number of discharge/recharge cycles
Longevity	% of original capacity after N cycles
Internal resistance	ohm
Efficiency	% of energy turned into heat
Bend radius	mm

Table 1. A number of battery characteristics. These are often in tension with each other – for example increasing recharge rate compromises longevity.

Such tradeoffs are present even within a given physical battery. For example, energy delivered by a battery in a single charge-discharge cycle (energy capacity) is inversely related to the rate at which the battery is drained (discharge rate). This is because the resistance losses inside a battery are proportional to the square of the current. Similarly, a battery's longevity – its ability to perform consistently following many charge-discharge cycles – is inversely related to the discharge and recharge rates. This is because higher currents speed up the creation of fissures in the electrodes that reduce the amount of energy a battery can store.

In summary, no single battery type can deliver the ever-growing list of requirements of modern devices: fast charging, high capacity, low cost, less volume, light in weight, less heating, better longevity, and high peak discharge rates.

A growing range of battery chemistries are under development, each of which delivers a different set of benefits in terms of performance. We believe that combining multiple of these heterogeneous batteries instead of using a single battery chemistry can allow a mobile system to dynamically trade between their capabilities and thereby offer attractive tradeoffs.

However, traditional methods of integrating multiple batteries are not suitable for heterogeneous batteries. Simply connecting them in series or parallel chains does not provide enough control over the flow of energy: batteries connected in series can only supply the same amount of current; batteries connected in parallel must operate at the same voltage and can only supply currents that are inversely proportional to their internal resistances.

We propose a new system, called Software Defined Battery (SDB), that allows heterogeneous batteries with different chemistries to be integrated in a mobile system. SDB consists of hardware and software components. The hardware enables fine-grained control of the amount of power passing in and out of each battery using smart switching circuitry. The charging and discharging hardware is designed to be low-cost, and hence the algorithmic complexity of computing how much power to draw from each battery, and how to recharge each battery, is placed in the SDB software that resides in the operating system (OS).

Deciding how much power to draw from each battery, and how to charge each battery is non-trivial. It depends on the efficiency of each battery under different workloads, the age of each battery, and also the user's workload and usage profile. For example, if a high power workload is anticipated in the future, then it could be worthwhile conserving charge on the battery that is more capable of handling such a workload in an efficient manner.

The SDB software component that resides in the OS implements a set of policies and APIs. The SDB software uses simple APIs to communicate with the SDB hardware. The algorithms implemented by this software use various metrics for increasing the single charge-discharge duration of the device, and the longevity of the batteries, and thereby decide the ratios in which to discharge each battery, and the ratios in which to charge them. We present the details of the APIs and policies in Section 3.

The SDB design is cross-layer and involves new chemistries, additional hardware, and new OS components. Although an alternative SDB implementation can be hardcoded in firmware, our cross layer approach has two main benefits. First, it opens up new battery parameters, previously unavailable to OS designers, for resource optimization. In existing mobile devices, the battery is usually treated as a black box, and is simply assumed as a reservoir of charge. As we show in Section 5, OS techniques yield substantial gains in battery usage. Second, this design allows a system designer to select any combination of batteries for an optimal design, including new chemistries as they are invented, and developed. All of these can be enabled through a software update.

Even with existing batteries, SDB enables several new scenarios, such as:

Bendable batteries for long-lived wearable devices: Bendable batteries are appealing for wearable form factor devices. For example, thin, bendable batteries can be installed in the straps of a smart watch to augment a traditional Li-ion battery in the body, and significantly improve battery life. However, these batteries are much less efficient than traditional Li-ion batteries because their rubber-like electrolyte increases internal resistance. Using SDB, we develop a prototype hybrid battery system using a bendable battery and a Li-ion battery, and develop an algorithm that a smart-watch OS can use to minimize the inefficiency in such a system based on user workload.

Supporting high power workloads: SDB enables two such scenarios. First, SDB enables a fast charging battery to be used in combination with a high energy density battery. A device can then gain a good percentage of its charge in just a few minutes, without losing out on total battery capacity or the longevity of the battery back. Second, SDB supports higher turbo modes for the CPU using a high power density battery in combination with a high energy density battery. SDB helps the OS decide when to enable higher turbo modes based on workload requirements, and also to intelligently manage the batteries.

Battery management for 2-in-1s: In 2-in-1 laptops that have a detachable keyboard, external battery packs under the keyboard are typically used to charge the main internal battery. This however, reduces the efficiency and effective energy capacity because of the losses involved in charging one battery from another. With SDB it is possible to reduce this inefficiency and improve effective energy capacity by up to 22%.

We discuss these in more detail in Section 5.

2. Background

Lithium-ion (Li-ion) batteries are commonly used in today's battery-powered electronic devices. In this section, we first present some basics of Li-ion batteries, and then describe how existing systems manage these batteries.

2.1 Battery Technologies

A Li-ion battery contains a negative electrode (the anode), which is usually made of carbon in graphite form, and a positive electrode (the cathode), which is typically a metal oxide. A separator ensures physical separation between the anode and the cathode to prevent shorting, and the battery is filled with an electrolyte composed of a lithium based salt whose ions can easily pass through the separator. Current is discharged when the electrodes are connected externally over a resistive load while positive Lithium ions flow from the anode to the cathode through the electrode and separator. During charging, Li-ion batteries store energy by trapping positive lithium ions in the anode when an external potential is applied, which is larger than the potential between the electrodes.

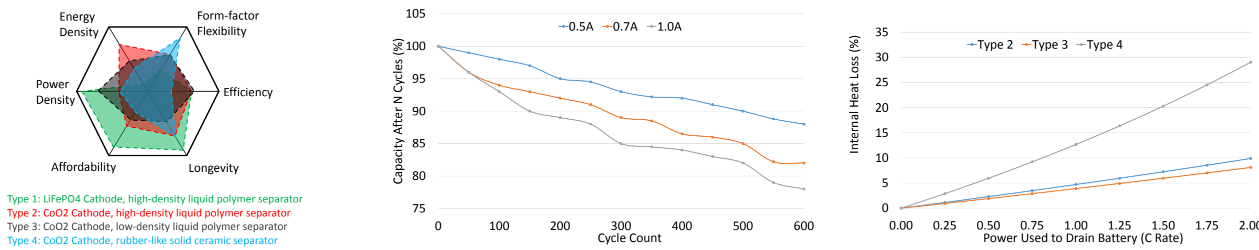

(a) Li-ion batteries compared (b) Charging rate affects longevity (c) Discharging rate vs. lost energy

Figure 1. Li-ion Battery Properties

Li-ion battery capabilities, such as longevity, energy density, and internal resistance, are largely determined by the materials used for the electrodes and the separator. The battery's gravimetric and volumetric energy densities are affected by the strength of the separator. The resistance of the battery, and hence its inefficiencies, depend on the resistance of the separator, which typically increases with the age of the battery. The power density of the battery is also affected by aging. The structural integrity of the electrodes determines how much energy they can store – some Lithium ions get permanently trapped in the anode. The anodes can develop cracks as they age, which can ultimately reduce both energy and power densities because Lithium ions get permanently trapped within the cracks. The material used for the electrode determines the initial energy and power densities, and also the expected longevity.

Figure 1(a) demonstrates the capabilities of four popular Li-ion batteries, which differ in the chemistry of materials used for the cathode and the separator. All four batteries have graphite as their anode.

Batteries of Type 1 are typically used in powered tools that need to charge quickly and provide high power for a short duration of time while not requiring a large energy capacity. Such batteries are a poor choice for mobile devices because of their poor energy density – a Type 1 battery is usually double the volume of a Type 2 battery with the same energy capacity. Type 2 batteries are commonly used in most mobile devices today. We measure the loss in capacity with respect to number of charge-discharge cycles for a sample Type 2 battery, and observe that the battery degrades much faster when discharged at higher current values, as shown in Figure 1(b).

Type 3 batteries are an emerging variation over Type 2 that have a slightly higher power density at the expense of some energy density. This is achieved by making the separator less dense allowing more Lithium ions to pass through per unit time. However, to retain enough strength to separate the electrodes, the weight of the separator is kept the same and this usually leads to decreased energy density as separators cannot store energy – only the electrodes can. Finally, Type 4 is another emerging battery that is flexible and bendable because of the physical properties of the rubber-like (ceramic-based) separator used – while the electrodes are implemented by coating material along the cell's walls. Unfortunately, such separators increase the resistance to passage of ions and thereby result in reduced power density and higher inefficiency, as shown in Figure 1(c).

2.2 Typical Power Management

Figure 2 shows a block diagram of the typical power management hardware. It consists of a (i) Battery (ii) Fuel gauge (iii) Battery charger, and (iv) Voltage regulator.

A *Battery pack* has one or more battery cells. Multiple cells are used to achieve higher voltage or higher capacity. While such multi-cell configurations exist today [2, 20–22], these cells have the same chemistry are either connected in series, parallel or a combination thereof. They are treated as a single monolithic battery by the OS. Our aim is to use a heterogeneous set of cells and achieve wide dynamic characteristics by exposing the cells directly to the OS.

The *Fuel gauge* keeps track of the state of charge (SoC) of the battery by measuring the voltage across the battery terminals, and the current flowing in and out of it. This information is exposed to the OS to take coarse grain actions based on SoC.

The *Battery charger* charges the battery with an appropriate charging current profile based on the battery's state of charge, the terminal voltage (the potential difference between the anode and the cathode), and the power source. An example charging profile looks like: the battery is charged at a constant high current until SoC reaches 80% (for example), and the charging is limited to a trickle charge or low current after the SoC reaches beyond 80%. Such profiles help ensure that the battery is not damaged given that higher currents tend to be damaging to the anode beyond a certain SoC.

Due to the battery's internal resistance R, the battery terminal voltage changes with the load current I due to the IR voltage drop. The internal resistance and the battery voltage themselves change with the amount of charge left in the battery. The job of the *Voltage Regulator* is to hide these terminal voltage variations due to changing potentials at the electrodes and the changing internal resistance and present a constant voltage to the load. The regulator also helps the processor implement Dynamic Voltage and Frequency Scaling (DVFS) by adjusting it's output voltage. Mobile devices

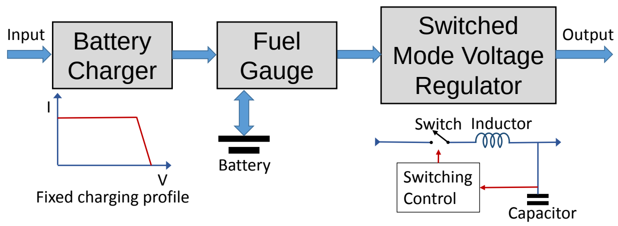

Figure 2. The traditional power management hardware

use switched mode voltage regulators due to their high efficiency. As the name implies, a switch mode power supply contains a switch that opens and closes to transfer packets of energy from the battery to an inductor. The inductor's voltage is smoothed using a capacitor (figure 2). A control loop maintains a constant voltage under varying load currents by changing the energy per packet or the packet switching frequency.

Typically, all these modules are contained in a single integrated circuit called a Power Management Integrated Circuit (PMIC) in a mobile device. The PMIC communicates with the OS over a serial bus. In current designs, the interactions between the OS and PMIC are limited to *query* operations, such as inquiring about remaining charge in the battery, terminal voltage or the cycle count. These parameters are exposed through the Advanced Configuration and Power Interface (ACPI). However, none of these APIs allow the OS to set the battery parameters, and in particular to change the amount of charge to be drawn from or provided to each cell within a battery pack. Through the SDB system, we propose enabling fine grain control over the behavior of these hardware sub modules by exposing a richer software API to the OS to dynamically change the amount of charge to be drawn from or provided to each battery.

3. SDB Design

SDB allows a device to use diverse batteries through fine-grain control of the amount of charge flowing in and out of each battery. SDB provides APIs to the OS to change the aforementioned power values based on user workload. We describe the SDB system in detail in this section.

3.1 System Overview

The SDB system spans components across three layers: the batteries and their chemistry, the battery management circuit, and the operating system. We outline these components and their interactions in Figure 3.

SDB allows a system designer to combine diverse batteries. The particular batteries chosen depend on the scenario, such as a fast charging battery and a high energy battery for a tablet, or a bendable battery and high energy battery for a smart-watch. We describe some of these combinations in Section 5.

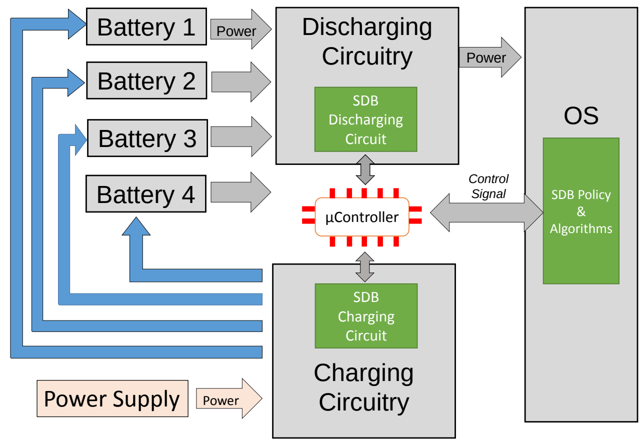

Figure 3. SDB System Overview

However, combining different battery types is not trivial. These batteries might have different capacities, and different terminal voltages at various states of charge. Therefore, we propose a new hardware architecture for charging and discharging. We design a new power distribution circuit for fine-grain control of how multiple batteries are discharged to support system load. A microcontroller interfaces between this power distribution circuitry and the mobile device OS to control the charging and discharging of batteries accordingly.

To enable flexibility in design, and to allow quick changes in policy, we only implement the mechanisms in hardware, and all policies are managed and set by the OS. A runtime component in the OS monitors the applications, the charging and discharging behavior of the users, and accordingly sets policies that meet user expectations from the mobile device in terms of daily battery life, longevity of the battery-pack and also performance of the CPU as we demonstrate in Section 5.

3.2 SDB Hardware

The SDB hardware needs to support discharging and charging across multiple, heterogeneous batteries.

For discharging, it has to provide a flexible mechanism for fine grain control of how the load current is supplied from each battery. This should support two things: coarse grain *switching* of the load across multiple batteries where the total load is supplied by a particular battery for an extended period of time; and the fine grain *sharing* of the load where a certain fraction of the load is drawn from each battery.

For charging, the SDB hardware has to support control over how batteries are charged. In contrast to existing solutions where batteries are charged according to a fixed charging profile, SDB requires setting of charging currents and charging profiles dynamically based on OS policies. Under certain circumstances, it should even be possible to charge a battery from another one.

Designing these flexible charging and discharging circuits are challenging for two reasons. First, due to the high currents that flow in these circuits, any electronic component in series with the current flow will cause energy losses. Hence, these circuit designs should introduce as few of these components as possible. Second, each extra component we introduce can increase the weight, volume and bill of material (BoM) cost of the device, which will make the proposed solution unattractive in the highly competitive hardware market.

3.2.1 SDB Discharging Circuit Design

A simple discharging circuit can be implemented using a combination of an electronic switch and a capacitor as shown in figure 4(a). The microcontroller achieves load switching by connecting the appropriate battery to the load. To achieve load sharing, the load is switched between the batteries at a high frequency in round-robin fashion. The ratio of the current draw is determined by the fraction of time the switch is connected to a particular battery. The capacitor acts as an energy store to smooth out the discontinuities due to switching. Parasitic battery capacitance and external capacitors smooth out the high frequency battery current.

However, this naive implementation has two main drawbacks. First the switch, typically implemented using a Field Effect Transistor (FET), has a finite on resistance that causes significant power loss at high load currents. Second, a switch with high power handling capability and the necessary capacitors increase the BoM cost and space required.

To overcome these shortcomings, we designed a new switched mode regulator architecture that integrates fine-grain battery switching into the regulator itself. As shown in discharging side of Figure 4(c), we restructure the built-in switch to achieve voltage regulation and support switching between multiple batteries – by drawing packets of energy from the batteries in a weighted round-robin fashion. We reuse the storage capacitor to smooth out the load current variations due to switching. We have evaluated the correctness of the proposed solution under different battery voltages and load conditions by running LTSPICE [25] simulations that accurately simulate the internals of the switch mode regulators. A more in-depth discussion on the correctness of the proposed solution under varying conditions is beyond the scope of this paper.

3.2.2 SDB Charging Circuit Design

The SDB charging circuit should have the ability to charge batteries at a configurable rate and also charge them from each other. Given that such charging should be possible irrespective of the battery voltage, the batteries should be connected through a buck-boost regulator, such that the energy source is at the input and the energy sink is at the output of the regulator. A buck-boost regulator is a particular form of switching regulator where the regulator output voltage can be either less than or greater than its input voltage.

Apart from charging batteries from each other, it should also be possible to charge all batteries from an external power supply. Typically, the external supply voltage is greater than the battery voltage, and buck regulators–a form of switched mode regulator whose output voltage is smaller than the input voltage–are used for charging the batteries.

Apart from different charging configurations, SDB requires dynamic fine grain control over the charging profile. This is achieved by instrumenting each switched mode regulator with multiple charging profiles where the SDB microcontroller dynamically selects the appropriate charging profile based on OS policy decisions.

Figure 4(b) shows how these modules can be combined to implement a flexible charging circuit. However, a major drawback of this configuration is the large number of switching regulators ($O(N^2)$ for N batteries) required, which negatively impacts the device BoM cost and space requirements.

We use a special characteristic of synchronous buck regulators–a form of buck regulator with superior current switching characteristics– to design a much simpler battery charging circuit. By appropriately controlling specific parameters, a synchronous buck regulator can be operated in reverse buck mode where the current can be made to flow from the output of the buck regulator to its input while maintaining a large voltage at the input (specific details of this reverse mode operation is beyond the scope of this paper).

Figure 4(c) shows the optimized charging circuit which requires only $O(N)$ switched mode regulators to charge N batteries. When an external supply is present, the microcontroller configures both R_1 and R_2 in *buck* mode to charge the batteries. When external power is removed, R_1 and R_2 are disabled. When B_2 is to be charged from B_1, R_1 operates in *reverse buck* mode while R_2 operates in *buck* mode and vice versa.

3.3 SDB Policies and APIs

Tradeoff	Description
Charge Power vs. Longevity	Higher charge rate quickly charges the battery, but results in faster internal crack formation leading to reduced cycle count.
Discharge Power vs. Longevity	Higher discharge rates support high current workloads, but reduced cycle count.
Discharge Power vs. Battery Life	Higher discharge power causes higher DC Internal Resistance (DCIR) losses that are proportional to the square of the current.

Table 2. Tradeoffs impacting SDB policies.

Our current SDB software architecture is illustrated in Figure 5. An *SDB Runtime* encapsulates the SDB microcontroller from the rest of the OS. The SDB Runtime is re-

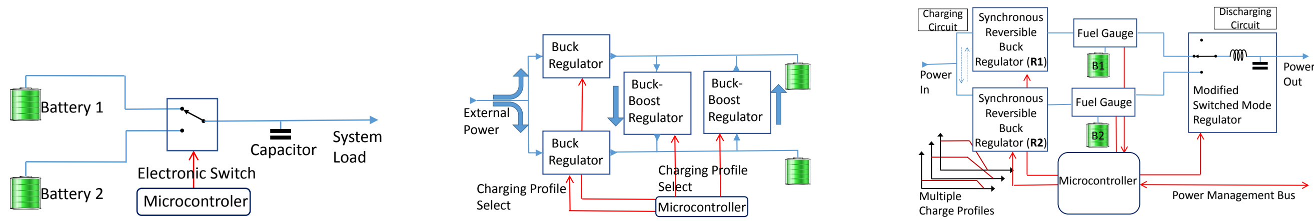

(a) Naive discharging circuit (b) Naive charging circuit (c) SDB hardware

Figure 4. (a) A simple switch and capacitor-based battery switching and sharing solution. (b) A naive implementation of a flexible charging circuit consisting of 2 buck regulators and 2 buck-boot regulators with dynamic charging parameters. (c) SDB hardware architecture for an example 2-battery system. The switched mode regulator implements discharge across multiple batteries, and the reverse buck regulators implement charge.

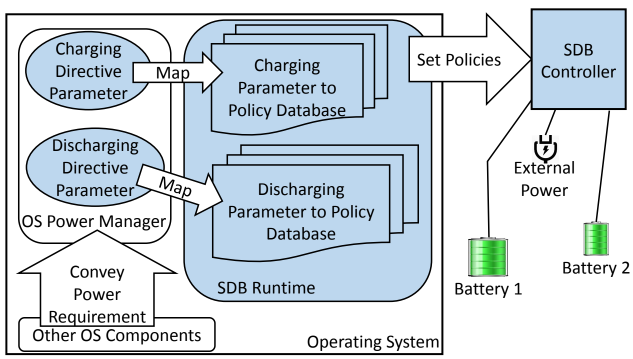

Figure 5. SDB software architecture

sponsible for all scheduling decisions affecting the charging and discharging of batteries. It takes clues from the rest of the OS, and communicates the charging and discharging scheduling decisions to the SDB controller.

APIs: For a system with N batteries, the SDB Runtime maintains two N-tuples $(c_1, \ldots, c_N)$ and $(d_1, \ldots, d_N)$ of non-negative values, one for charging and one for discharging. In both cases, the N values add up to one and represent power ratios; i.e., the numbers represent the fraction of power that must go in and out of each of the N batteries. The runtime communicates with the SDB microcontroller using the following four APIs:

- `Charge(`c_1`, `c_2`, ..., `c_N`)`: Charge N batteries in proportion to c_1, c_2, ..., c_N, when being charged from an external source.
- `Discharge(`d_1`, `d_2`, ..., `d_N`)`: Discharge N batteries in proportion to d_1, d_2, ..., d_N, when being discharged.
- `ChargeOneFromAnother(`X`, `Y`, `W`, `T`)`: Charge battery Y from battery X with a power of W for time T.
- `QueryBatteryStatus()`: Returns an array with state of charge, terminal voltages and cycle counts for each battery.

The SDB Runtime affects changes in the charging and discharging behavior by adapting the $2N$ numbers and sending them to the microcontroller using the above APIs, which enforces the ratios. Such changes can be triggered for example by a change of the user's needs, the battery state, workload patterns, or external factors such as a change in device temperature etc. Determining optimal battery charging/discharging policies is non-trivial, and the underlying algorithmic problems are deep and interesting. Often, various battery properties are in tension with one another. For example, fast-charging a battery all the time can greatly accelerate its aging. Other such tradeoffs are given in Table 2. In this paper, we only scratch the surface of these algorithmic problems and instead describe a set of natural policy heuristics that exhibit good albeit non-optimal performance.

Metrics: Two key metrics any charging/discharging policy seeks to optimize are *Cycle Count Balance* (CCB) and *Remaining Battery Lifetime* (RBL). The RBL metric simply captures the remaining battery lifetime of the device, assuming that no further charging occurs in the future. In other words, RBL is the amount of useful charge in the batteries. The CCB metric reflects that–ideally–the charging and discharging policies should maximize longevity of the device, by balancing the charging cycles of each battery. In a heterogeneous battery system each battery is a unique precious resource that excels on a few metrics of interest described in Table 1. Therefore, having a metric like the CCB ensures that these batteries are aging such that the properties of a battery that the user is most interested in are preserved over time. For example, a battery that has the ability to charge fast must be treated as a precious resource for a user who relies on fast charging during low-battery situations.

Concretely, let χ_i be the number of charging cycles tolerable by battery i before its capacity drops below some acceptable threshold, and let cc_i be the number of charging cycles of battery i. The *wear-ratio* $\lambda_i = cc_i/\chi_i$ describes what fraction of the tolerable recharge cycles have already been consumed by battery i. We define CCB as the ratio $CCB = \max_i \lambda_i / \min_j \lambda_j$, i.e., the ratio between the most and least worn-out battery, normalized to each battery's total tolerable cycle count. A device's longevity is maximized by balancing CCB.

Charge/Discharge Algorithms: The heuristics currently driving our SDB Runtime are simple and driven by the following observation: It is possible to derive charging and discharging algorithms that (in isolation!) optimize the CCB and the instantaneous RBL metric. We use these four "optimal" algorithms (CCB-Charge, RBL-Charge, CCB-Discharge, and RBL-Discharge) and weigh them by means of two parameters–Charging and Discharging Directive Parameter–handed to the SDB Runtime by the rest of the OS. Essentially, these parameters guide the SDB Runtime to weigh one of the algorithms more heavily at any moment in time. For example, a low value of the Charging Directive Parameter indicates that the user is in no hurry (e.g. charging at night), and that the Runtime should prioritize the use of the CCB-Charge algorithm. On the other hand, a high value of this parameter would lead the Runtime to prioritize the RBL-Charge algorithm in order to increase the useful charge (and thus the remaining battery lifetime) in the batteries as quickly as possible - say just before boarding an airplane. The discharge scenario is similar.

The CCB-Charge and CCB-Discharge algorithms are simple. These policies essentially enforce the controller to schedule the batteries (either for charging and discharging) in such a way that the resulting CCB is minimized i.e. is as close to 1 as possible. Our RBL-algorithms are more interesting. Consider the discharge case, and let $y_1, \ldots, y_N$ be the amount of current drawn from each of the batteries. The key underlying insight is that we can maximize the instantaneous RBL of the battery system by minimizing the total resistance losses across all the batteries. This can be achieved *if the resistances of the batteries are proportional to the square-root of their DCIR-to-SoC ratios*. Thus, the RBL-Discharge algorithm seeks to allocate the currents $y_1, \ldots, y_N$ in such a way that the effective resistances of batteries are as much as possible proportional to the square-root of their DCIR-to-SoC rates minimizing the total energy wasted through resistive losses. Mathematically speaking, let δ_i be the instantaneous derivative of battery i's DCIR curve, and let R_i be the current resistance. Then, the RBL-Discharge algorithm balances $R'_i = \sqrt{\delta_i/\lambda}$, where $R'_i = R_i + \delta_i y_i$ and λ is a Lagrangian multiplier constant. Again, the case for charging (RBL-Charge) is similar. The SDB runtime calculates these power values at coarse granular time steps and updates the ratios based on the DCIR-SoC curves given by the manufacturer of the batteries.

A word of caution is necessary. The above RBL-algorithms are "optimal" only in an instantaneous sense. They minimize the instantaneous decrease of RBL (when discharging), or maximize the instantaneous increase of RBL (when charging). However, they are not globally optimal. Across the length of an entire workload, these algorithms might not actually maximize battery lifetime as we show in Section 5; i.e., if we had knowledge of the future workload, we could improve upon the above instantaneously-optimal algorithms by making temporarily sub-optimal choices from which the system can profit later, e.g., keeping a battery fully charged, if we know that this battery will be particularly helpful in the way of CCB or RBL for a future workload. For example, the overall cycle life or daily battery life may be improved when compared to using instantaneous mechanisms all the time.

Exploring these and other algorithmic nuances is interesting, but beyond the scope of this paper. We just note that the SDB resource optimization problem differs from traditional resource scheduling mechanisms, such as for Big.Little processors, hybrid storage, and SSD wear leveling, because of the resource in question – batteries. The main focus of traditional resource management algorithms is to multiplex a resource efficiently across a number of entities, such as users, processes, virtual machines or erase blocks in case of SSDs over some fixed periods of time. The challenge of battery resource scheduling is threefold: daily battery life cannot be simply extended by minimizing instantaneous power losses; their long-term cycle life cannot be simply extended by balancing cycle life across batteries. Knowledge of impending workload can be used to improve the latter two metrics by picking strategies that may not be an instantaneous optimums as we demonstrate in Section 5. We hope that exposing the appropriate APIs will help system and algorithm designers to customize the scheduling algorithms for their battery configuration, and user workloads based on predicted as well as expected user behavior.

4. SDB Prototype & Microbenchmarks

In this section we describe the implementation of SDB and present microbenchmarks to evaluate it.

4.1 SDB Hardware Prototype

We built a hardware prototype of the SDB hardware architecture in Figure 4(c). Figure 7 shows the components of our prototype.

We built a custom controller board with a ARM Cortex M3 microcontroller, a low-loss switching circuit, and a Bluetooth wireless link. We also built a custom fuel gauge module that consists of a coulomb counter and a controller. We modified an off-the-shelf battery-charger evaluation board to enable dynamic charge current setting by the microcontroller on the control board. These hardware modules were interconnected as shown in figure 7.

We highlight several key differences between our prototype and the proposed hardware solution. First, due to the difficulty of making hardware connections directly to the power management serial bus on our experimental devices, we use a Bluetooth wireless connection to interface between the microcontroller and the SDB runtime in the OS. We power the Bluetooth radio module on the hardware prototype

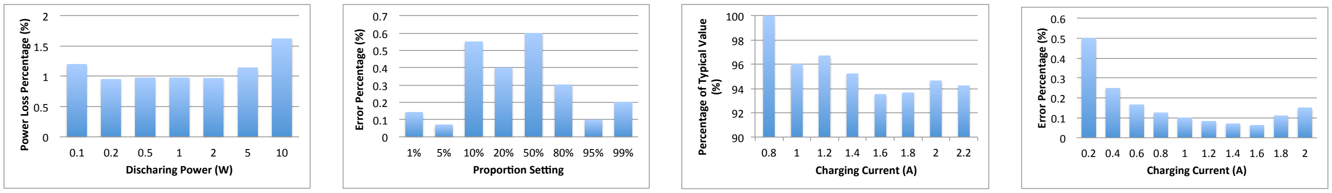

(a) The % power loss of the discharge circuit vs discharge power

(b) The % error of the measured % discharge current vs the % discharge current set by the microcontroller.

(c) Efficiency of the charging circuit as a % of the typical efficiency of the charging chip vs charging current.

(d) The % error of the measured charging current vs the charging current set by the microcontroller

Figure 6. SDB Hardware Microbenchmarks

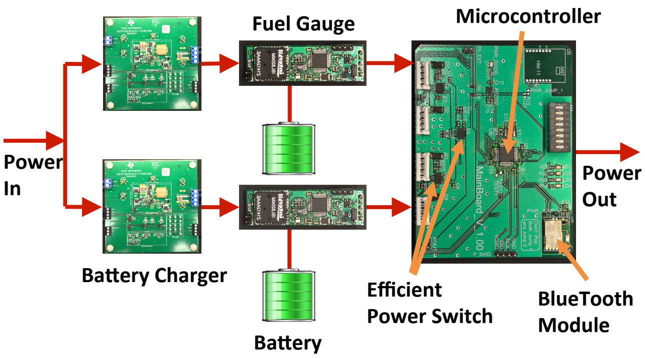

Figure 7. SDB Prototype Implementation

using an external power source to eliminate any interference with results.

Since it is difficult to modify the existing switched mode regulators to achieve fine-grain current sharing, we used an ideal diode to switch between the batteries. The switching between batteries is extremely fast, and hence the battery sees a constant, smooth current draw. We note that the small power-loss due to this switch underestimates the efficiency achievable by the proposed solution. As mentioned in section 3, the extra power-loss and the high component cost can be eliminated by augmenting existing switching regulators to switch across multiple batteries.

The boards were designed with Altium Designer [1], a circuit board development package.The firmware was written in C using the IAR for ARM V7.40 tool chain. The board firmware contains $\simeq$ 3500 lines of code. We also developed the prototype SDB Runtime shown in Figure 5 with 1200 lines of code.

We conducted simulations and microbenchmark experiments to evaluate the efficiency and accuracy of our hardware design, as well as to evaluate the correctness of the firmware and the runtime. Circuit simulations were done in LTSPICE [25], a simulation program with integrated circuit emphasis (SPICE). We generated the circuits shown in Figure 4 in LTSPICE, and conducted extensive simulations at various power loads to validate system correctness, stability, and responsiveness.

4.2 Hardware Microbenchmark results

We conducted several microbenchmark experiments to evaluate the efficiency and accuracy of our hardware. We measured currents and voltages using a Fluke 8846A 6.5 Digit Multimeter and an Agilent DSO-X 2004A Oscilloscope. We computed power loss of a module by multiplying the voltage drop across the module by the current flowing though it. We used an Agilent E3640A Power Supply to power the circuit.

We first evaluate the efficiency of the discharge circuit due to battery switching and sharing. Figure 6(a) plots the power loss vs the load power of the discharge circuit. We observe that the power-loss remains $\simeq$ 1% under typical light loads while it reaches 1.6% with a 10W load. We note that these numbers are likely to become negligible when the switching and sharing capability is integrated into the regulator as proposed in Figure 4(c).

We next evaluate battery sharing accuracy of the discharge circuit based on the discrepancy between the load current assigned to a battery and the actual measured current draw from the battery. Figure 6(b) plots the error of the measured currents vs the proportional current draw assignment. We observe that our implementation has $< 0.6\%$ error under a wide range of current assignments.

Next we evaluate the performance of the charging circuit. Since the charging efficiency has an upper bound on the efficiency of the actual chip used, we report the measured efficiency of our implementation compared with the typical efficiency of the battery charging chip as reported by the chip data sheet. Figure 6(c) plots this efficiency under different charging load conditions. We observe that our solution has very high efficiency at light loads and the charging efficiency reaches $\simeq$ 94% at high charging currents.

Next we evaluate the charging current accuracy. Figure 6(d) shows the error of the measured charging current vs the charging current set by the microcontroller for one of the batteries. We observe that, even under low charging currents requiring fine-grain control, the error remains at or below 0.5%.

We developed an SDB emulator to not only facilitate OS researchers to easily conduct experiments but also to obtain repeatable experiments that helped us in debugging SDB policies without damaging real batteries.

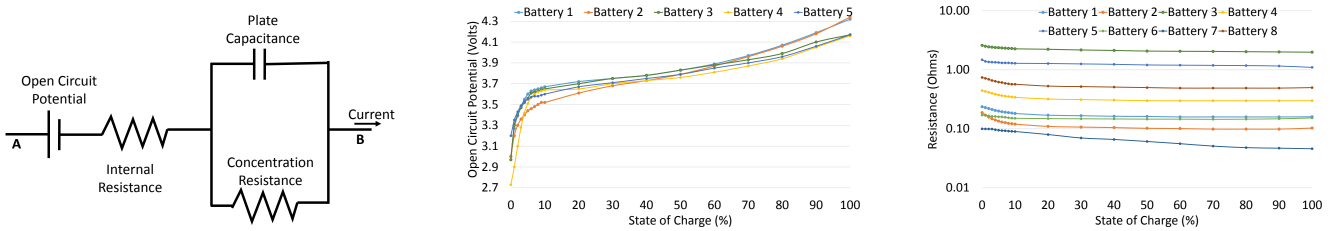

(a) Battery Model (b) Open Circuit Potential (c) Internal Resistance

Figure 8. Battery Simulator: (a) Battery modeled with four variables that are learned using experimentation: Open circuit potential, internal resistance, concentration resistance and plate capacitance. This model allows us to conduct experiments in a scalable manner. (b) The open circuit potential of a battery increases with the state of charge (amount of energy left) of the battery. (c) The internal resistance of a battery decreases with the state of charge.

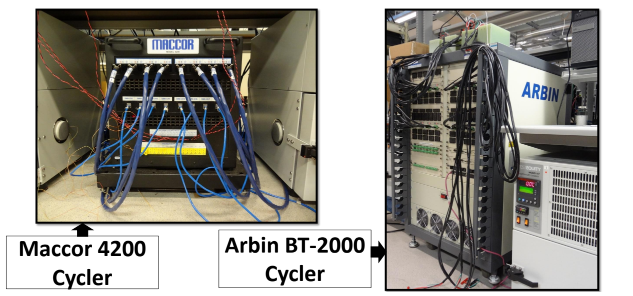

Figure 9. Battery testers used for modeling 15 different state-of-the-art batteries developed for usage in mobile devices.

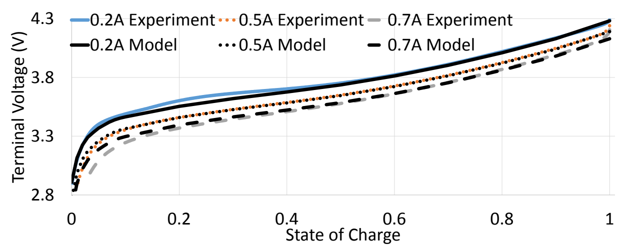

Figure 10. Validating the model against battery testing hardware reveals that our model is 97.5% accurate.

4.3 SDB Emulator

We build a multi-battery emulator to evaluate the benefits from SDB. We emulate several kinds of batteries' behavior including their charging and discharging characteristics. We build a model for batteries based on Thevenin's Model as built by other battery researchers [7, 8, 11, 15, 18] to simulate batteries used in production devices. The simplified Thevenin model is reproduced in Figure 8(a). The model has four parameters: open circuit potential, internal resistance, concentration resistance and plate capacitance.

The open circuit potential of a battery is the voltage across the terminals of the battery when no load is applied. It increases with the amount of energy left in a given battery. Figure 8(b) plots the open circuit potential of a few batteries as the energy left in them increases.

The internal resistance of a battery is the resistance across the terminals of the battery when a load is applied. It decreases with the amount of energy left in a given battery. Figure 8(c) plots the resistance of a few batteries as the energy left in the them increases.

The concentration resistance and the plate capacitance of a battery are fixed values for a given battery. We measure the open circuit potential, internal resistance, concentration resistance and the plate capacitance for several kinds of batteries. We use the industry standard Arbin BT-2000 [3] and Maccor 4200 [26] battery cycling and testing hardware (shown in Figure 9) for measuring the battery properties. These systems allow us to send a configurable amount of power in and out of the batteries and accurately measure the open circuit potential, internal resistance, concentration resistance and the plate capacitance at fine time scales.

The model takes the initial SoC, OCP vs SoC, resistance vs SoC, concentration resistance, and plate capacitance to emulate a battery. At each time step, based on the SoC, it estimates OCP and resistance. Using the updated values, it calculates the values for the SoC after the time step.

We build the battery model using a few batteries and validate the models against other batteries of the same type whose data is extracted using the testing hardware shown in Figure 9. The validation results for one of the batteries is shown in Figure 10. We measure the terminal voltage using the battery testing hardware when various currents are applied and validate the actual values against the model's estimations of the terminal voltage. The terminal voltage is the voltage across points A and B in Figure 8(a). The results show that our model is accurate to 97.5%. We modeled 15 batteries in total: Two of Type 4, two of Type 3, eight of Type 2 and 3 more of other types (refer to Figure 1(a)).

We emulate the SDB hardware using the battery emulators. We implement a simple software layer that takes the input power requirement and splits it across a given number of batteries according to the power policies set by an OS. The model and the SDB emulator are integrated into the OS (for devices instrumented with power meters) using 4,800 lines of code across modules written in C#, Python and Matlab.

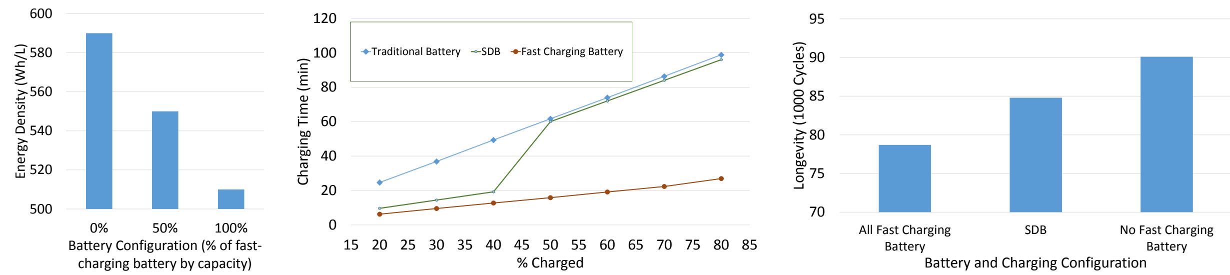

(a) Energy Density Comparison (b) Charge Time Comparison (c) Longevity Comparison

Figure 11. Energy density vs charge speed vs longevity tradeoff: (a) Energy density decreases as the proportion of fast-charging battery capacity increases. (b) Charge time behavior with varying charging speeds as the proportion of fast-charging battery increases. (c) SDB presents a middle ground between the extremes provided by pure high-density or pure fast-charging batteries.

We focus on three hardware platforms: a tablet, a phone and a watch. The tablet is a "2-in-1" development device with Intel Core i5 CPU, 4GB DRAM, 128GB SSD, 12 inch display. The phone is a Qualcomm development device with Snapdragon 800 chipset, 1GB DRAM, 4 inch display. The watch is a Qualcomm Snapdragon 200 development board with hardware similar to several smart-watches [35, 36]. These devices are instrumented to obtain fine grained (100 Hz) power-draw measurements. The power-draw is then fed into the emulator to calculate the energy drawn from the batteries.

5. SDB Applications

In this section we describe three scenarios that benefit from using SDB with heterogeneous batteries. We also show how SDB policies can be customized for the different scenarios, and demonstrate the benefits of integrating future workload knowledge in the SDB system.

5.1 Adopting High Power-Density Batteries

High power-density batteries reduce charging times. Compared to the traditional Li-ion batteries, they also provide higher instantaneous power to CPUs, which can then dynamically increase frequency and reduce latency for applications. However, their efficiency and longevity decreases as power increases. Therefore these characteristics must be dynamically balanced via SDB to meet user expectations.

Charging Behavior: The amount of time a device takes to charge affects its usability. A device that takes several hours to charge fully is less usable. Likewise, a device that needs to be charged every few hours is not useful. Batteries have to be designed such that they last through the day for typical use yet support fast charging. From a chemistry point of view, energy density (both volumetric and gravimetric) is in a tussle with power density. This means that batteries that are able to pack more joules in a given weight/volume charge less quickly, and vice versa. This leaves device designers with three incompatible scenarios: Get as much energy capacity as possible and not offer state-of-the-art charging speeds, or offer great charging speeds albeit at lesser capacity, or meet capacity and charging speed goals but increase the volume and/or weight of the battery.

SDB can offer several attractive tradeoffs between these three extremes by allowing device designers to combine a fast-charging battery with a high energy-density battery. Consider a device that is constrained by volume, such a device can dedicate half of its capacity budget to a fast-charging battery and another half to a high energy-density battery. This allows the device to attain the following tradeoff: Obtain close to 50% of charge really quickly yet lose only a small portion of energy capacity.

We demonstrate how an OS can exploit tradeoffs between longevity, energy capacity and charging speeds that SDB enables. We measure longevity as the capacity of the battery after a given cycle count compared to the original capacity. For example, a battery that loses 30% of its capacity after 1,000 cycles has a longevity score of 70 after 1000 cycles. The cycle count increases each time the battery is charged to more than 80% (cumulative) of current energy capacity. For example, if a user charges the battery to 50% and drains it to 0%, the cumulative charge counter is set to 50. Later when the user charges the battery again beyond 30%, the cumulative charge counter is increased to 80, the cycle count is incremented and the cumulative charge counter is set to zero until the next time the device is charged. Each time the battery reaches 100% capacity, the total energy that it absorbed is noted as its current capacity. Longevity is an important metric for device designers, since it is typically included in the device's warranty.

Charging speed, measured in minutes, is the time it takes a battery to go from 0% SoC to a given capacity. For example, if a battery takes 100 minutes to charge from 0 to 50% (of original capacity) then its charging speed is given as 100 minutes for 50%.

We showcase the benefits of SDB using a simple setup, in which we meet the total capacity requirement of the device, of 8000 mAh, using 0%, 50%, and 100% from a high energy density battery. So, the first case is two cells of the high energy density battery, the third is two cells of only the high power density battery, and the second is a mix of both. The energy density of several high energy-density batteries we benchmarked is between 590–600 Wh/l. The energy density of the high power-density batteries we benchmarked is between 530–540 Wh/l. However, these batteries are prone to expand in size when charged with high currents. Therefore, the effective energy density is between 500–510 Wh/l. This allows the 50% configuration to have an effective energy density between 545–555 Wh/l as shown in Figure 11(a).

Through Figure 11 we highlight the compromises when picking homogeneous batteries, and show that SDB can help. We pick the charging parameter for the SDB Policy to charge the batteries as quickly as possible. Figure 11(b) shows the charging speeds for several capacity targets. The results show that the SDB enabled 50% mechanism allows device designers to achieve an attractive tradeoff: By losing less than 7% energy capacity, a device can obtain 40% of the charge in three times less duration compared to a traditional no fast charging battery setting. Users constrained by charging speeds typically also have a time deadline. For example, a user getting on an airplane would like to get as much charge as quickly as possible in short span may not be able to charge the battery to a 100% anyway and therefore this makes it an attractive tradeoff to have.

Figure 11(c) shows longevity of the three configurations after 1000 cycles. Here again, it is clear that SDB presents a middle-ground between losing only 10% of capacity after 1000 cycles with slow charging speeds vs. losing close to 22% of capacity for 100% fast charging batteries [33].

Discharging Behavior: Modern Intel CPUs (both Atom and Core series) are capable of automatically overclocking on the basis of power supply and temperature restrictions to reduce the latency of computations. However, batteries that are not capable of supplying high power for long duration restrict the amount of time an Intel CPU can go into turbo mode, and this can affect interactive and latency sensitive applications. Equipping a device with a battery that has higher power capabilities can unlock higher frequencies for longer duration of time.

Modern Intel CPUs have three active power levels: Long term system limit, burst limit and battery protection limit [23]. The long term system limit is the power level that is maintained during regular usage. However, short bursts (up to three minutes) of higher power limit allow the CPU to reach higher frequencies for better performance. The three minute limit is imposed to avoid overheating. However, even higher power can be used for higher performance. The CPU goes into this power level only for a few milliseconds every second to avoid damaging batteries that are not designed to supply high power for long duration – traditional Li-ion battery for example. We propose augmenting the traditional

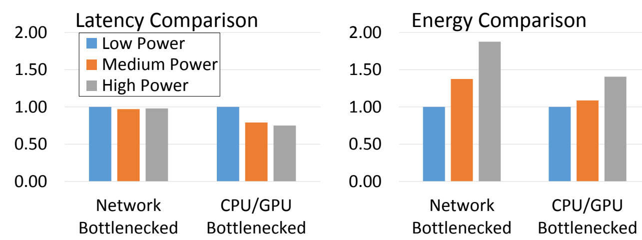

Figure 12. Comparing performance priority levels. Each priority level provides a different kind of latency vs. energy tradeoff for different kinds of applications. This creates an opportunity for a workload-aware OS to match priority levels to tasks to obtain the best possible benefits.

Li-ion battery with a high power-density battery to support increased amounts of time spent in the highest power level to reduce latency for certain tasks. The parameter design is again straightforward in this case. As the value increases, the power manager first informs the runtime of higher power requirements and then subsequently informs the CPU firmware of higher power availability.

However, higher frequencies may not always benefit application performance. A fixed parameter value would not be ideal for all situations. Consider these two extreme users for example: (1) A user who mostly uses network facing applications like email, browsing, social networking, audio and video calls and (2) A user who extensively uses the local CPU and GPU resources for gaming and development. Latest 2-in-1 tablet/laptops strive to be unified devices that suits both such users.

We compare three parameter values for these users: low, medium and high. In the low level, the high power-density battery is disabled and the CPU is informed of the decreased power capacity. Medium level is one where both batteries are enabled but the CPU is allowed to draw the same amount of peak power from both batteries – which is twice the peak power of the high energy-density battery. High priority level is one where the CPU is allowed to draw maximum possible power from both the batteries. We calculate latency and energy benefits of running the two user profiles at these three priority levels and plot the results in Figure 12

Networked bottlenecked applications' energy consumption increases when the Turbo capabilities of a CPU increase without noticeable latency benefits. We find that the energy required for a network bottlenecked workload increases by up to 20.6% with no noticeable reduction in latency for higher parameter values. Extra energy is used by the CPU for entering higher turbo frequencies when the task is bottlenecked by network and also because of the higher losses in the battery because of higher power draw. However, increased Turbo capability from the high power-density battery does lead to latency benefits for computationally bottlenecked tasks.

We find that the PassMark and 3DMark benchmarks obtain up to 26% better scores on individual tests (integer math, floating math, rendering, fractals and GPU computations). A fixed parameter value is therefore not a good solution. The operating system must dynamically increase the value for compute bottlenecked applications to improve latency and reduce the value for network bottlenecked tasks for energy savings.

5.2 Adopting Flexible Batteries

Flexibility and bendability are important structural properties for wearable devices, e.g. a watch-strap that is flexible and bendable tends to be easier to wear. Coincidentally, there are a few emerging battery chemistries that enable bendability. The bendability, unfortunately, comes at the cost of other battery properties. Such batteries use a solid (rubber-like) electrolyte in place of a traditional liquid (polymer) electrolyte. Unfortunately, the solid (elastic) state of the electrolyte increases the resistance for the Li-ions and therefore, such batteries have higher internal losses. Several prototype bendable batteries we tested are excellent at handling low power workloads but often are very inefficient for high power workloads.

SDB can enable a scenario where a small traditional Li-ion battery in smart-watches is augmented with bendable batteries. This helps design better wearables that utilize the strap space to increase capacity but are still able to execute high power workloads like GPS tracking while running and cycling. The reduction in the size of the rigid Li-ion battery also allows for the design of a less bulky watch body.

The bendability of the battery in the strap is a boon, but its low efficiency is a bane that has to be intelligently managed to maximize effective battery life of the device. It is important to preserve energy in the efficient battery for times when the user is expected to perform power-intensive tasks. For example, the user may exercise, run or bicycle during certain times of the day, which all require high power. Therefore, the SDB policies should preserve the efficient battery for such times.

Since smart-watch usage will vary across users, we compare two extreme parameter values to demonstrate the benefits of SDB: One that minimizes instantaneous losses by drawing appropriate amounts of power from both the batteries and one that draws higher amounts of power from the inefficient battery to conserve the efficient battery.

Figure 13 demonstrates the setting and the results. We use a 200mAh Li-ion battery in combination with a 200mAh bendable battery for the setting. For a typical user who spends the entire day checking messages on his smart-watch and goes for a run in the evening, we plot the workload and the instantaneous losses in the batteries. We find that the latter method minimizes the total losses and therefore increases overall battery life by over an hour. These results provide evidence that mobile OSes that are aware of a user's day to day schedule may be able to provide better battery life by setting the right parameter. On the other hand, it is interesting to note that if the user had not gone for a run then the first policy would have given better battery life suggesting that the knowledge of an impending workload can help save energy in heterogeneous battery settings.

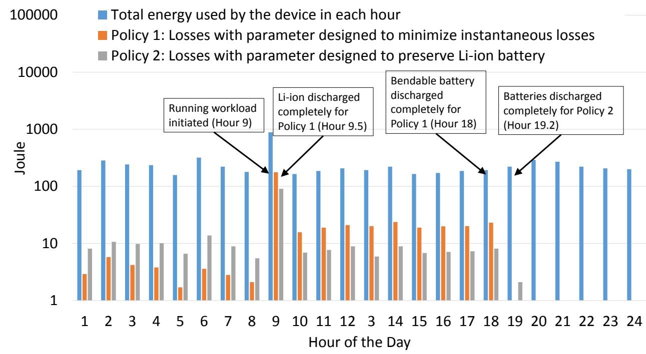

Figure 13. Fixed priority levels are bad. Priority levels have to be changed according to expected user schedules and workloads.

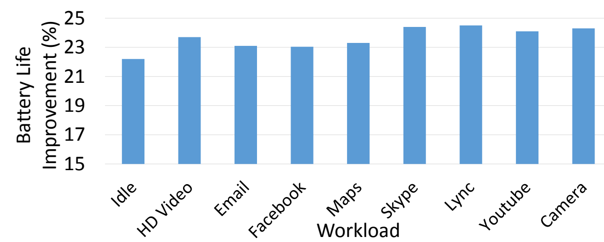

Figure 14. Drawing power simultaneously from internal and external batteries is more energy efficient than depleting the external battery for conserving and charging the internal one.

5.3 Battery Management for 2-in-1s

2-in-1 devices are tablets that have a detachable keyboard. Some such devices have another battery under the keyboard [39]. In such a setting, there are two batteries exposed to the OS, often with different capacities but the same internal chemistry – traditional Li-ion. However, efficiency of the battery in the base is less as it is used solely to charge the battery in the tablet. Significant amount of energy is lost in charging the internal battery with the external one, yet the reason why device manufacturers have chosen this route is to simplify design.

SDB via the OS can improve the battery life of a combined internal and external battery by understanding user behavior and expectations. The power drawn from an external battery can either be used towards running the system, for charging the main battery or both. For a user who rarely unplugs an external battery, the better solution would be to draw power simultaneously from both batteries as the internal losses are proportional to the square of the current (resistive losses = I^2R). Splitting the power draw across the two batteries, therefore, reduces the internal losses and increases the energy delivered to the system.

However, this strategy may not be ideal for a user who mostly operates in tablet-only mode. For such users, it makes more sense to draw as much power for as long as possible from the external battery to handle system load and also for charging the internal battery.

The OS sets a low parameter value for times when the external battery is expected to be plugged in for longer duration while high parameter values are for times when the external battery is plugged during battery crises.

Figure 14 shows the comparison of two extreme parameters for various application workloads on a development 2-in-1 device with two equal sized traditional Li-ion batteries. Results show that the parameter causing simultaneous power draw from both batteries provides 22% more battery life than the parameter that causes one battery to charge another. However, this gain is not realizable for a user who only keeps the base with the secondary battery plugged in for short periods of time. The OS must, therefore, learn, predict and adapt to user behavior to set appropriate parameters.

6. Related Work

A large body of research has investigated techniques to improve the battery life of mobile devices. Prior work has focused on application specific optimizations [29, 44], system-level frameworks for accounting [10, 13, 29–32, 34, 45, 46], system-level energy optimizations [19], network protocol optimizations, technological improvements, programming language techniques, better measurement and analysis techniques [4–6, 14, 28, 37, 41, 43]. Through SDB, we investigate a new technique to improve battery life by leveraging multiple batteries, and by reducing the inefficiencies in the source of energy of mobile devices – the battery.

Multi-cell systems where smaller cells of different sizes and shapes are connected in series, parallel or a combination thereof to form a larger battery are fairly common [2, 20–22]. Modern battery management and measurement hardware from Texas Instruments [40] and Maxim [27] are able to manage such batteries using technology developed for single-celled batteries. This is because similar cells that are connected in series or parallel collectively behave more or less like a larger cell. However, these techniques do not work when the batteries are heterogeneous. SDB provides a way to integrate and manage the diverse, heterogeneous batteries using separate fuel gauges, and new hardware and software to control the power flowing in and out of each battery.

Multiple battery systems where one battery is used to charge the primary battery are fairly common [12, 24, 39]. Such situations arise in mobile systems when external battery packs are used to charge the main battery. Different battery types have been explored for electric vehicles as well. However, existing proposals use these multiple batteries in an either-or fashion where the vehicle is powered using only one battery at a time. Similarly, recent research [17, 42] has investigated the use of multiple battery types and power sources, in different power hierarchies, to shift the peak power demand in data centers [17, 42]. As we show in Section 5, it is possible to get significantly more battery life by using SDB's technique of intelligently drawing portions of power from each battery.

7. Discussion

Hardware vs. the OS: There are three main benefits of performing policy management in the OS instead of the microcontroller firmware. First, the OS has access to knowledge that can help design better policies as shown in Section 5, such as access to users' calendar and appointments. Policies can be better tailored to the user's schedule. For example, if the OS (via smart assistants such as Siri, Cortana and Google Now) knows that user is about to board a plane then it might make sense to charge as quickly as possible and take the hit to longevity. Second, embedding the complexity in the OS reduces the cost of the SDB microcontroller. Third, it is much simpler to dynamically upgrade policies, and the accompanying code, in the OS instead of the microcontroller firmware.

Cost of SDB: We believe the BoM cost and space requirement of our SDB solution will not be significant. We add parts by replacing similarly sized components, therefore weight and volume is not a concern. The proposed charging and discharging circuit can be integrated with a few extra gates in a traditional PMIC. Finally, most mobile devices have a microcontroller that performs power management. We expand the functionality of one such controller for implementing the SDB controller. As stated before, having multiple homogeneous cells to form a larger battery pack [2, 20–22] is fairly common. We propose using heterogeneous cells instead of homogeneous ones and exposing them to the OS. Therefore, there is no additional cost or bulk because of SDB.

Benefits to Single Battery Systems: A few concepts of SDB are applicable to single battery systems as well. For example, the tradeoffs of increased turbo capabilities and how quickly to charge (or discharge) such that the cycle count longevity requirements are met, are useful for single battery systems. Also, the workload-based loss reduction mechanism is also applicable for homogeneous, multi-cell battery packs.

8. Conclusions & Future Work

Device requirements are typically hard to meet with a single battery since these requirements are often in conflict with each other. We present the SDB system that allows a device to use multiple heterogeneous batteries, and get the best of all of them. The SDB hardware is designed to be low cost, and provides rich functionality to the OS. The SDB APIs allow an OS to dynamically route charge to, and from the batteries based on application workload such that the overall goals (battery life, cycle count, fast charge, etc.) are met. We show several new scenarios that can be enabled with SDB, and demonstrate its feasibility using a prototype, and detailed emulations.

Moving forward, we are taking the SDB work in two main directions. First, we are tying personal assistants like Siri [38], Cortana [9], and Google Now [16] with SDB. These assistants understand user behavior and the user's schedule and by using this information, an OS can perform better parameter selection. For example, if the user's profile suggests that the user plays video games in the evening, then it SDB could preserve a higher power-density battery for that workload. Second, we are working on additional devices that would benefit from this technology, such as drones, smart glasses, and electric vehicles (EV). Each would require a different combination of battery chemistries, and the SDB logic might be different too. For example, an EV's NAV system could provide the vehicle's route as a hint to the SDB Runtime, which could then decide the appropriate batteries based on traffic, hills, temperature, and other factors. Our preliminary analysis shows that SDB might help these systems achieve tradeoffs that until now were considered to be at odds with each other.

9. Acknowledgments

We would like to thank the anonymous SOSP reviewers and also our shepherd Luis Ceze. We would also like to thank Bojun Huang for his contributions and fruitful discussions.

References

[1] Altium Designer. http://www.altium.com/altium-designer/overview.

[2] Apple MacBook (2015) Battery Design. http://www.apple.com/macbook/design/.

[3] Arbin BT-2000 Battery Testing Equipment. http://www.arbin.com/products/battery.

[4] N. Balasubramanian, A. Balasubramanian, and A. Venkataramani. Energy consumption in mobile phones: A measurement study and implications for network applications. In *Proc. IMC'09*, Chicago, Illinois, Nov. 2009.

[5] J. Bickford, H. A. Lagar-Cavilla, A. Varshavsky, V. Ganapathy, and L. Iftode. Security versus Energy Tradeoffs in Host-Based Mobile Malware Detection. In *Proc. 9th ACM MobiSys*, Washington, DC, June 2011.

[6] A. Carroll and G. Heiser. An Analysis of Power Consumption in a Smartphone. In *Proc. USENIX ATC*, Boston, MA, June 2010.

[7] M. Chen and G. A. Rincon-Mora. Accurate Electrical Battery Model Capable of Predicting Runtim and IV Performance. *IEEE Trans. Energy Conversion*, 21(2):504–511, 2006.

[8] C.-F. Chiasserini and R. R. Rao. Energy efficient battery management. *IEEE Journal. Selected Areas in Communications*, 19(7):1235–1245, 2001.

[9] Cortana Personal Assistant. https://www.windowsphone.com/en-us/how-to/wp8/cortana/meet-cortana?signin=true.

[10] M. Dong and L. Zhong. Self-Constructive High-Rate System Energy Modeling for Battery-Powered Mobile Systems. In *Proc. 9th ACM MobiSys*, Washington, DC, June 2011.

[11] O. Erdinc, B. Vural, and M. Uzunoglu. A dynamic lithium-ion battery model considering the effects of temperature and capacity fading. In *Proc. IEEE International Conference on Clean Electrical Power*, Capri, Italy, June 2009.

[12] External Battery Packs. http://www.ianker.com/External%20Batteries/category-c1-s1.

[13] J. Flinn and M. Satyanarayanan. Energy-Aware Adaptation of Mobile Applications. In *Proc. 17th ACM SOSP*, Charleston, SC, Dec. 1999.

[14] R. Fonseca, P. Dutta, P. Levis, and I. Stoica. Quanto: Tracking Energy in Networked Embedded Systems. In *Proc. 8th USENIX OSDI*, San Diego, CA, Dec. 2008.

[15] L. Gao, S. Liu, and R. A. Dougal. Dynamic lithium-ion battery model for system simulation. *IEEE Trans. Components and Packaging Technologies*, 25(3):495–505, 2002.

[16] Google Now. http://www.google.com/landing/now/.

[17] S. Govindan, A. Sivasubramaniam, and B. Urgaonkar. Benefits and Limitations of Tapping into Stored Energy for Datacenters. In *ISCA*, 2011.

[18] H. He, R. Xiong, X. Zhang, F. Sun, and J. Fan. State-of-Charge Estimation of the Lithium-Ion Battery Using and Adaptive Extended Kalman Filter Based on an Improved Thevenin Model. *IEEE Trans. Vehicular Technology*, 60(4):1461–1469, 2011.

[19] B. D. Higgins, J. Flinn, T. J. Giuli, B. Noble, C. Peplin, and D. Watson. Informed Mobile Prefetching. In *Proc. 10th ACM Mobisys*, Low Wood Bay, United Kingdom, June 2012.

[20] iFixit Galaxy Tab 2 10.1 Teardown: 25.9 Wh battery with two cells (Step 10). https://www.ifixit.com/Teardown/Samsung+Galaxy+Note+10.1+Teardown/10144.

[21] iFixit iPad Air 2 Teardown: 32.9 Wh battery with cells (Step 17). https://www.ifixit.com/Teardown/iPad+Air+2+Teardown/30592.

[22] iFixit Surface Pro 3 Teardown: 42.4 Wh battery with four cells (Step 13). https://www.ifixit.com/Teardown/Microsoft+Surface+Pro+3+Teardown/26595.

[23] Intel Active CPU Power Levels. http://www.intel.com/content/dam/www/public/us/en/documents/presentation/advancing-moores-law-in-2014-presentation.pdf.

[24] iPhone Battery Case. http://www.mophie.com/shop/iphone-5/juice-pack-helium-iphone-5.

[25] LTSpice: Linear Technologies Simulator Program with Integrated Circuit Emphasis.

[26] Maccor 4200 Battery Testing Equipment. http://www.maccor.com/Products/Model4200.aspx.

[27] Maxim Fuel Gague for Mobile Devices. http://para.maximintegrated.com/en/results.mvp?fam=batt_stat&295=Fuel%26nbsp%3BGauge&1379=ModelGauge.

[28] A. P. Miettinen and J. K. Nurminen. Energy Efficiency of Mobile Clients in Cloud Computing. In *Proc. 2nd USENIX HotCloud*, Boston, MA, June 2010.

[29] R. Mittal, A. Kansal, and R. Chandra. Empowering Developers to Estimate App Energy Consumption. In *Proc. 18th ACM MobiCom*, Istanbul, Turkey, Aug. 2012.

[30] A. Pathak, Y. C. Hu, and M. Zhang. Where is the energy spent inside my app?: Fine Grained Energy Accounting on Smartphones. In *Proc. EUROSYS*, Bern, Switzerland, Apr. 2012.

[31] A. Pathak, Y. C. Hu, M. Zhang, P. Bahl, and Y.-M. Wang. Fine-Grained Power Modeling for Smartphones using System Call Tracing. In *Proc. 6th ACM EUROSYS*, Salzburg, Austria, Apr. 2011.

[32] F. Qian, Z. Wang, A. Gerber, Z. M. Mao, S. Sen, and O. Spatschek. Profiling Resource Usage for Mobile Applications: a Cross-layer Approach. In *Proc. 9th ACM MobiSys*, Washington, DC, June 2011.

[33] Qualcomm Quick Charge. https://www.qualcomm.com/products/snapdragon/quick-charge.

[34] A. Roy, S. M. Rumble, R. Stutsman, P. Levis, D. Mazieres, and N. Zeldovich. Energy Management in Mobile Devices with Cinder Operating System. In *Proc. 6th ACM EUROSYS*, Salzburg, Austria, Apr. 2011.

[35] Samsung Galaxy Gear Specs. http://www.samsung.com/us/mobile/wearable-tech/SM-V7000ZKAXAR.

[36] Samsung Gear Live and Gear 2. http://www.gizmag.com/samsung-gear-live-vs-gear-2-smartwatch-comparison/32775/.

[37] A. Shye, B. Scholbrock, and G. Memik. Into the wild: Studying real user activity patterns to guide power optimizations for mobile architectures. In *Proc. 42nd IEEE MICRO*, New York, NY, Dec. 2009.

[38] Siri Personal Assistant. https://www.apple.com/ios/siri/.

[39] Surface Power Cover. http://www.microsoft.com/surface/en-us/support/hardware-and-drivers/power-cover.

[40] Texas Instruments Fuel Guages for Mobile Devices. http://www.ti.com/lsds/ti/power-management/battery-fuel-gauge-products.page#p1152=SingleCell&p338=Li-Ion/Li-Polymer&p199=I2C&o4=ACTIVE&p626max=2000;29000&p626min=100;100&p1960=&p2192=&p2954=DSBGA.

[41] N. Thiagarajan, G. Aggarwal, A. Nicoara, D. Boneh, and J. P. Signh. Who Killed My Battery: Analyzing Mobile Browser Energy Consumption. In *Proc. WWW*, Lyon, France, Apr. 2012.

[42] D. Wang, C. Ren, A. Sivasubramaniam, B. Urgaonkar, and H. Fathy. Energy storage in datacenters: what, where, and how much? In *ACM SIGMETRICS*, 2012.

[43] Y. Wang, J. Lin, M. Annavaram, Q. A. Jacobson, J. Hong, B. Krishnamachari, and N. Sadeh-Koniecpol. A Framework for Energy Efficient Mobile Sensing for Automatic Human State Recognition. In *Proc. 7th ACM Mobisys*, Krakow, Poland, June 2009.

[44] F. Xu, Y. Liu, T. Moscibroda, R. Chandra, L. Jin, Y. Zhang, and Q. Li. Optimizing Background Email Sync on Smartphones. In *Proc. 11th ACM MobiSys*, Taipei, Taiwan, June 2013.

[45] C. Yoon, D. Kim, W. Jung, C. Kang, and H. Cha. AppScope: Application Energy Metering Framework for Android Smartphones using Kernel Activity Monitoring. In *Proc. USENIX ATC*, Boston, MA, June 2012.

[46] L. Zhang, B. Tiwana, Z. Qian, Z. Wang, R. P. Dick, Z. M. Mao, and L. Yang. Accurate online power estimation and automatic battery behavior based power model generation for smartphones. In *Proc. 8th IEEE/ACM/IFIP CODES+ISSS*, Taipei, Taiwan, 2010.